

# The onset of a liquid-vapour transition in metallic nanoparticles

G. Bilalbegović and H. O. Lutz

*Fakultät für Physik, Universität Bielefeld, D-33615 Bielefeld, Germany*

(May 15, 2017)

## Abstract

We study lead nanodroplets containing 147 to 1415 atoms at temperatures ranging from the bulk melting point up to the beginning of the evaporation regime. Molecular dynamics simulation and an embedded atom potential are used. The structures, total energies, and mobility of atoms in the clusters are analyzed. We found that the liquid cluster of 147 atoms shows a pronounced tendency to form non-spherical shapes, and sometimes separates into two droplets. Bigger clusters disassemble by evaporation of monomers. We also explore shape oscillations of these nanodroplets using the nuclear liquid drop model.

arXiv:cond-mat/9710034v1 [cond-mat.mtrl-sci] 3 Oct 1997

## I. INTRODUCTION

Clusters assembled from metal particles are scientifically interesting and technologically important [1]. Physical phenomena in clusters of atoms and molecules do not necessarily have the same features as in bulk phases. Melting of metal clusters was already studied by computer simulations [1–7], and in experiments [1,8–10]. In contrast, the studies of clusters at even higher temperatures, i.e., approaching the liquid-vapour transition are scarce. Exceptions are early Monte Carlo and Molecular Dynamics (MD) simulations for very small Lennard-Jones clusters that extended to the temperature region of the vapour phase [11–14]. Related simulations were also performed in the field of nuclear fragmentation [15], and recently in the study of fragmentation for argon clusters [16]. Understanding the behavior of nanoparticles at such high temperatures may also shed light onto the process of achieving plasma and controlled fusion in a gas of clusters [17].

Melting of lead clusters of sizes ranging from a few to about 100 nm were investigated by high-sensitivity optical reflectance and dark-field electron microscopy [10]. Spherical and non-spherical nanometric Pb inclusions in inert amorphous matrices of *SiO* and *Al<sub>2</sub>O<sub>3</sub>* were studied and it was found that melting is enhanced by surface and curvature effects. These studies have been carried out up to the bulk melting point of lead:  $T_{sl} = 600.56$  K, while the liquid-vapour transition temperature for bulk lead is:  $T_{lv} = 2033.16$  K.

In this letter we present a MD simulation study for liquid magic number Pb clusters containing 147, 309, 561, and 1451 atoms. The high-temperature structures, total energies, the mean-square displacements, and diffusion of atoms are analyzed. A calculation of shape oscillations for lead nanodroplets in the liquid drop model has been carried out.

## II. METHOD AND COMPUTATIONAL DETAILS

Properties of metals in bulk, surfaces and clusters are unlikely to be described well within the MD method without a many-body potential [18]. We have used such a classical many-body potential for lead [19–21]. The set of parameters in the potential was determined by fitting to several measured properties of metal [22]. This potential was already used in MD simulations of the structural and vibrational properties of lead clusters [19,20]. The bulk melting point for the potential is  $T_{sl} = 618 \pm 4$  K [21]. This value was precisely determined by simulating coexisting liquid and solid phases under constant energy. For the present investigation of the high-temperature behaviour of nanoparticles we have estimated the bulk liquid-vapour transition temperature as  $T_{lv} \sim 2050$  K. The precise calculation of the liquid-vapour transition temperature for a given potential is in principle and computationally more involved (in comparison with the calculation of the bulk melting point) and will be discussed elsewhere.

In this simulation lead atoms were at  $T = 0$  K distributed as regular Mackay icosahedra [23] of 147, 309, 561, and 1415 particles. In reference [19], the authors find using the same potential that at  $T = 0$  face-centered cubic morphologies are favoured over icosahedra. This is the result of the low surface energy anisotropy between Pb(111) and Pb(100), and of the high tensile surface stress which inhibits icosahedral structure. However, at  $T > 0$  the stress decreases and icosahedra become more favoured. In experiments with argon clusters and in simulations for clusters described by pair potentials (such as Lennard-Jones and

Morse), there is now clear evidence that for less than 1500 atoms icosahedra are more stable than fcc structures [24,25]. The situation is less clear for metallic clusters. The majority of experimental and theoretical studies find that icosahedral clusters are also energetically preferred for metallic clusters of less than 1500 atoms, even at  $T = 0$  [26,4]. Actually, the morphology of the energetically preferred structure for solid clusters at low temperature is not important for our study of liquid nanoparticles at high temperatures. Due to our wish to compare the results of simulations with future experimental studies of melting and evaporation we have chosen icosahedra as starting point in our simulation. As in other MD simulations of metal clusters [2–7] no boundary conditions have been employed. A time step of  $7.33 \times 10^{-14}$  s was used. MD simulations with damped dynamics were first performed to extract the kinetic energy until the clusters reached the structure corresponding to a local energy minimum. Then the clusters were heated up to temperatures ( $T < 2000$  K) where evaporation of atoms starts within a typical time scale of classical MD simulations. The embedded atom potentials are known to show realistic evaporation, i.e., to be much less prone to enhanced evaporation during MD simulation in comparison with the pair potentials. First the “heating” runs at constant temperature were carried out for  $5 \times 10^4$  time steps. Because of the difficulties in achieving equilibrium in the liquid temperature region, rather long runs of  $10^6$  time steps (i.e., 7.3 ns) were used to calculate the cluster properties. The temperature was controlled by rescaling the particle velocities at each time step. Note that the potential used here (and other embedded atom potentials) are not applicable at extremely high temperatures, for example at  $T > 2000$  K and approaching plasma conditions. These potentials are not fitted for this temperature region and the resulting low atomic coordination.

### III. RESULTS AND DISCUSSION

#### A. Structures and mobility

The equilibrium shape of a macroscopic liquid metal drop is a sphere because of the negligible anisotropy of the liquid-vapour interface free energy in comparison with the one of the solid-vapour interface. We have found that on the simulation time scale the liquid clusters exhibit substantial shape fluctuations at high temperatures. This tendency towards transient formation of non-spherical shapes decreases with increasing cluster size, but it is still present even for the largest cluster of 1415 atoms studied here. We may mention that non-spherical shapes were also found in experimental studies of nanometric lead inclusions [10]. A snapshot of atomic positions producing a very elongated lead droplet is presented in Fig. 1 (a). In the further time evolution this cluster separates into two smaller droplets as shown in Fig. 1 (b). The colour of the atoms reveals that the cluster emits a small subcluster. The process presented in Fig. 1 is the only occurrence we found (within our long, but limited simulation time) for a droplet separation into two parts, although several other extremely elongated shapes similar to Fig. 1 (a) were observed, especially for the smallest cluster and above  $T > 1000$  K. For most liquid droplets a typical process at these temperatures is single atom evaporation. A similar tendency of less intense evaporation for small as compared to large nanoparticles was recently found in a MD study of melting of argon clusters [27]. Another rare event - a dimer evaporation was also detected. We have

found that the number of evaporated atoms strongly depends on the length of time evolution during the MD simulation. For example, a liquid nanoparticle of 1415 atoms at  $T = 1600$  K completely vaporizes after  $3 \times 10^5$  time steps, whereas after  $10^5$  time steps only 4 atoms evaporate. For an almost immediate (within  $\sim 10$  ps) complete “explosive” disintegration of lead nanoparticles of these sizes much higher temperatures of the order of 5000 K are needed. However, as pointed out above, the reliability of the potential used is questionable in this temperature region.

In most bulk liquids the coordination number is  $\sim 8 - 11$ , i.e., it is smaller than the coordination number of, for example, 12 which is the property of close-packed bulk solid fcc metals [28]. In addition, as a result of surface effects, the average coordination number in clusters is always smaller than in the bulk. The average coordination numbers for all liquid nanoparticles studied here at several temperatures are given in Table I. Our calculation of the coordination numbers (and other cluster properties which we present below) extends to the beginning of the evaporation regime, i.e., up to  $T = 1200$  K. We found that at  $T = 1000$  K and  $T = 1200$  K, after several nanoseconds, one or two atoms evaporated from the liquid clusters of 309, 561, and 1415 atoms. After such an evaporation process, the calculations were continued only for the remaining liquid cluster. From Table I one can see how the average coordination number roughly increases with cluster size and decreases with temperature.

Steps in the caloric curve are a signature of melting [1–7]. We also studied the potential energy per atom,  $E$ , as a function of temperature from melting up to the evaporation regime. It was found that the  $E = f(T)$  function is linear for all studied nanoparticles in that temperature region.

Atomic configurations presented in Fig. 1 show the mobility of the atoms on a qualitative level. The mean-square displacements for the clusters after several nanoseconds of simulation and at several temperatures are shown in Fig. 2. At lower temperatures ( $T < 1000$  K), the mean-square displacements rise approximately linearly with time. Such a behaviour is typical for liquid diffusion. Sharp increases at higher temperatures are the results of evaporation, or the onset of evaporation. As pointed out above, the atom which has evaporated (and moved from the surface of the nanodroplet at a distance larger than the cutoff radius of the potential, i.e.,  $> 5.6$  Å) is excluded from further consideration. Note that as a result of evaporation from the cluster of 561 atoms the mean-square displacements are bigger at 1000 K (560 atoms in the liquid cluster), than at 1200 K (559 atoms).

The diffusion coefficients of bulk solid and bulk liquid phases are orders of magnitude different ( $10^{-9} \text{ cm}^2\text{s}^{-1}$  vs  $10^{-5} \text{ cm}^2\text{s}^{-1}$ ). The temperature dependence of the diffusion coefficient of lead clusters is shown in Fig. 3. The values are typical for diffusion in the liquid phase. As for the mean-square displacements, a jump of the diffusion coefficient is the result of the onset of evaporation.

## B. Shape oscillations of liquid lead clusters

It is interesting to estimate the influence of the size of a lead nanodroplet on its shape oscillations. Many phenomena in cluster physics can be analyzed using the tools developed in nuclear physics [29]. For nuclei some phenomena, for example magic numbers, can only be studied within independent particle models. Other phenomena, for example binding

energies, vibrational properties, and fission of heavy nuclei, are studied using collective (continuum) models, such as the liquid drop model. Experimental and theoretical investigations have shown that the same two types of models can be applied for metallic clusters [29]. The fission measurements for small gold clusters were interpreted using the nuclear liquid drop model and the results indicated that the vibrational properties of metallic clusters, nuclei, and liquid drops are similar [30]. A common approach to the analysis of vibrational properties of clusters is either by direct diagonalization of the dynamical matrix, or by calculating the Fourier transform of auto-correlation functions in a MD simulation. For liquid clusters bigger than 100 atoms as studied in this work, these traditional approaches give a broad, structureless line in the frequency spectrum [31,20]. Instead, we analyze the shape oscillations of liquid lead nanoparticles using the nuclear liquid drop model [32]. In this model surface and volume modes are analyzed separately and the results are expressed by macroscopic properties of the metal. Three kinds of shape oscillations are possible: surface oscillations, modes of vibration involving compression, and coupled oscillations.

The distance of the surface of a slightly deformed liquid drop from the origin,  $R(\theta, \phi)$ , can be expanded as

$$R(\theta, \phi) = R_0 \left( 1 + \sum_{\lambda\mu} \alpha_{\lambda\mu} Y_{\lambda\mu}^*(\theta, \phi) \right), \quad (1)$$

where  $R_0$  is the equilibrium radius,  $\alpha_{\lambda\mu}$  are normal coordinates, and  $Y_{\lambda\mu}(\theta, \phi)$  are the spherical harmonics [32]. The equations of oscillatory motion are

$$\ddot{\alpha}_{\lambda\mu} + \omega(s)_\lambda^2 \alpha_{\lambda\mu} = 0. \quad (2)$$

Eigenfrequencies of the surface oscillations are given by

$$\omega(s)_\lambda^2 = \frac{\sigma \lambda (\lambda - 1) (\lambda + 2)}{\rho_0 R_0^3}, \quad (3)$$

where  $\sigma$  is the surface tension and  $\rho_0$  is the density [32]. In Eqs. (1)-(3), the value  $\lambda = 0$  represents a compression without change of shape, whereas  $\lambda = 1$  describes a translation of a droplet as whole. This can be seen by considering Eq. (1) and respectively, the volume of an incompressible drop and a small translation of the center of mass along the axis  $\theta = 0$ . Therefore, the lowest order surface oscillations are quadrupole modes  $\lambda = 2$ .

Compressional oscillations in liquid droplets also exist. Small deviations of the density  $\rho(\vec{r})$  which are solutions of the linearized hydrodynamical equations that lead to the wave equation are given by

$$\delta\rho(\vec{r}, t) = \rho_0 j_\lambda(k_{n\lambda} r) Y_{\lambda\mu}^*(\theta, \phi) \alpha_{n\lambda\mu}(t), \quad (4)$$

where  $j_\lambda$  is a spherical Bessel function. If the boundary condition is such that  $\delta\rho(\vec{r}, t)$  vanishes at  $r = R_0$ , then the eigenvalue equation is

$$j_\lambda(k_{n\lambda} R_0) = 0. \quad (5)$$

The compressional eigenfrequencies are given by

$$\omega(c)_{n\lambda} = u_c k_{n\lambda}, \quad (6)$$

where  $u_c$  is the sound velocity in the liquid.

The ratio of the eigenfrequencies of surface and compressional modes (Eqs. (3) and (6)) slowly decreases as the number of atoms in the cluster increases. In general, if the liquid cluster (or nucleus) is small, it is important to consider coupling of the surface and compressional modes. These coupled modes are solutions of the wave equation with a modified boundary condition such that the pressure induced by the shape oscillations is in equilibrium with the pressure induced by the compressional oscillations [32]. The corresponding eigenvalue equation of the coupled modes is

$$\frac{1}{j_\lambda(k_{n\lambda}R_0)} \left[ \frac{\partial}{\partial r} j_\lambda(k_{n\lambda}r) \right]_{r=R_0} = \frac{\lambda}{R_0} \frac{\omega(c)_{n\lambda}^2}{\omega(s)_\lambda^2}. \quad (7)$$

The surface, compressional, and coupled frequencies were calculated using the experimental data for bulk lead:  $u_s = 1800 \text{ ms}^{-1}$  [33],  $\rho_0 = 10678 \text{ kgm}^{-3}$  [34], and  $\sigma = 0.453 \text{ Nm}^{-1}$  [33]. The average radii of approximately spherical clusters were taken from configurations obtained in MD simulations at 600 K. The calculation shows that for these lead nanodroplets the frequencies of coupled modes are approximately equal to the frequencies of surface modes. The size dependence of the surface and compressional frequencies is presented in Fig. 4. Frequencies of compressional modes are of course bigger than the corresponding frequencies of surface modes. The frequencies increase with increasing value of  $\lambda$  and with decreasing size of the nanodroplets. This agrees with our results of MD simulations where the most pronounced shape oscillations were found for the smallest liquid cluster of 147 atoms.

These results provide for the first time an insight into the behavior of neutral liquid metal clusters at high temperatures, up to the beginning of the evaporation regime. Experimental investigations of clusters in this temperature range, either using optical, diffraction techniques, and mass spectroscopy [1,8–10], or cluster fragmentation properties [16,17,35] are desirable.

## ACKNOWLEDGMENTS

This work has been supported by the Volkswagen Foundation and the Deutsche Forschungsgemeinschaft.

## REFERENCES

- [1] Large Clusters of Atoms and Molecules, ed. T. P. Martin (Kluwer, Dordrecht, 1996).
- [2] F. Ercolessi, W. Andreoni, and E. Tosatti, *Phys. Rev. Lett.* **66** (1991) 911.
- [3] I. L. Garzon and J. Jellinek, *Z. Phys. D* **20** (1991) 235.
- [4] S. Valkealahti and M. Manninen, *Phys. Rev. B* **45** (1992) 9549.
- [5] O. H. Nielsen, J. P. Sethna, P. Stoltze, K. W. Jacobsen, and J. K. Nørskov, *Europhys. Lett.* **26** (1994) 51.
- [6] X. Yu and P. M. Duxbury, *Phys. Rev. B* **52** (1995) 2102.
- [7] L. J. Lewis, P. Jensen, and J. L. Barrat, *Phys. Rev. B* **56** (1997) 2248.
- [8] P. Buffat and J. P. Borrel, *Phys. Rev. A* **13** (1976) 2287.
- [9] T. P. Martin, U. Näher, H. Schaber, and U. Zimmermann, *J. Chem. Phys.* **100** (1994) 2322.
- [10] R. Kofman, P. Cheyssac, A. Aouaj, Y. Lereah, G. Deutscher, P. Cheyssac, T. Ben-David, J. M. Penisson, and A. Bourret, *Surf. Sci.* **303** (1994) 231.
- [11] J. K. Lee, J. A. Barker, and F. F. Abraham, *J. Chem. Phys.* **58** (1973) 3166.
- [12] R. D. Eppers and J. Kaelberer, *Phys. Rev. A* **11** (1975) 1068.
- [13] J. Kaelberer and R. D. Eppers, *J. Chem. Phys.* **66** (1977) 3233.
- [14] M. Rao, B. J. Berne, and M. H. Kalos, *J. Chem. Phys.* **68** (1978) 1325.
- [15] A. Vicentini, G. Jacucci, and V. R. Pandharipande, *Phys. Rev. C* **31** (1985) 1783.
- [16] V. N. Kondratyev, H. O. Lutz, and S. Ayik, *J. Chem. Phys.* **106** (1997) 7766.
- [17] T. Ditmire, J. W. G. Tisch, E. Springate, M. B. Mason, N. Hay, R. A. Smith, J. P. Marangos, and M. H. R. Hutchinson, *Nature* **386** (1997) 54.
- [18] M. S. Daw, S. M. Foiles, and M. I. Baskes, *Mater. Sci. Rep.* **9** (1993) 251.
- [19] H. S. Lim, C. K. Ong, and F. Ercolessi, *Surf. Sci.* **269/270** (1992) 1109.
- [20] H. S. Lim, C. K. Ong, and F. Ercolessi, *Z. Phys. D* **26** (1993) S45.
- [21] G. Bilalbegović, F. Ercolessi, and E. Tosatti, *Europhys. Lett.* **17** (1992) 333.
- [22] F. Ercolessi, M. Parrinello, and E. Tosatti, *Philos. Mag. A* **58** (1988) 333.
- [23] A. L. Mackay, *Acta Crystallogr.* **15** (1962) 916.
- [24] J. Xie, J. A. Northby, D. L. Freeman, and J. D. Doll, *J. Chem. Phys.* **91** (1989) 612.
- [25] J. P. K. Doye and D. J. Wales, *Z. Phys. D* **40** (1997) 466.
- [26] C. L. Cleveland and U. Landman, *J. Chem. Phys.* **94** (1991) 7376.
- [27] A. Rytkönen, S. Valkealahti, and M. Manninen, *J. Chem. Phys.* **106** (1997) 1888.
- [28] C. A. Croxton, *Statistical Mechanics of the Liquid Surface* (John Wiley, New York, 1980).
- [29] *Nuclear Physics Concepts in the Study of Atomic Cluster Physics*, eds. R. Schmidt, H. O. Lutz, and R. Dreizler (Springer, Berlin, 1992).
- [30] W. A. Saunders, *Phys. Rev. Lett.* **64** (1990) 3046 and references therein.
- [31] W. D. Kristensen, E. J. Jensen, and R. M. J. Cotterill, *J. Chem. Phys.* **60** (1974) 4161.
- [32] A. Bohr and B. R. Mottelson, *Nuclear Structure, Vol. II* (Benjamin, Reading, 1975).
- [33] G. W. C. Kaye and T. H. Laby, *Tables of physical and chemical constants*, (Longman, London, 1973).
- [34] WebElements, <http://www.shef.ac.uk/~chem/web-elements/>, (University of Sheffield, Sheffield, 1997).
- [35] U. Werner, K. Beckord, J. Becker, and H. O. Lutz, *Phys. Rev. Lett.* **74** (1995) 1962.

## TABLES

TABLE I. The average coordination numbers for liquid lead clusters of a given total number  $N$  of particles, calculated after 7.3 ns of simulation. If evaporated atoms exist their number is given in parentheses; they were excluded in the calculation of the average coordination number and other cluster properties.

Temperature (K)	$N = 147$	$N = 309$	$N = 561$	$N = 1415$
600	8.99	9.00	9.34	9.72
800	8.75	8.84	8.93	9.34
1000	8.44	8.43	8.94(1)	9.04
1200	8.41	8.13(1)	8.64(2)	8.88(2)



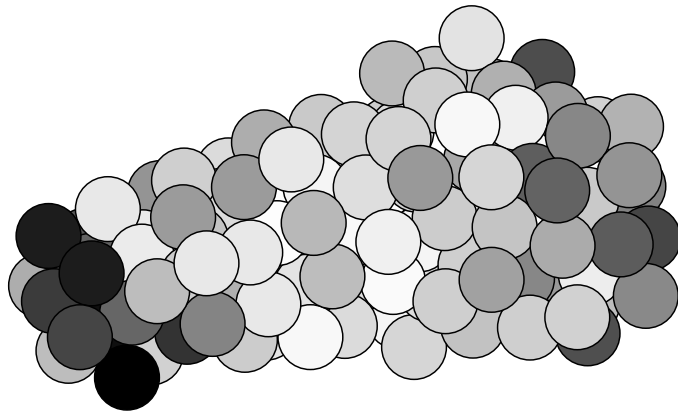
## FIGURES

FIG. 1. Atomic positions showing: (a) non-spherical shape of the liquid cluster of 147 atoms at  $T = 1300$  K after 6.96 ns of time evolution, (b) the same sample after 7.32 ns. The relative darkness of an atom is proportional to its square displacement during the run. Black particles are those with the maximum of mobility.

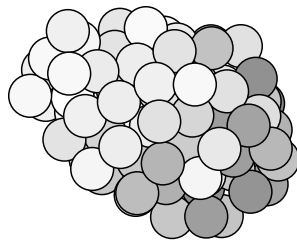
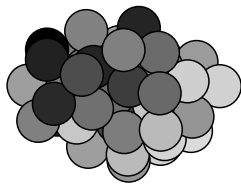
FIG. 2. Mean-square displacements for liquid lead nanoparticles at several temperatures: (a) 147, (b) 309, (c) 561, (d) 1415 particles.

FIG. 3. Diffusion coefficients for liquid lead clusters as a function of the temperature.

FIG. 4. Eigenfrequencies of lead nanodroplets in the liquid drop model as a function size: (a) surface oscillations, (b) compressional oscillations ( $n = 1$ ).



(a)



(b)

Fig. 1

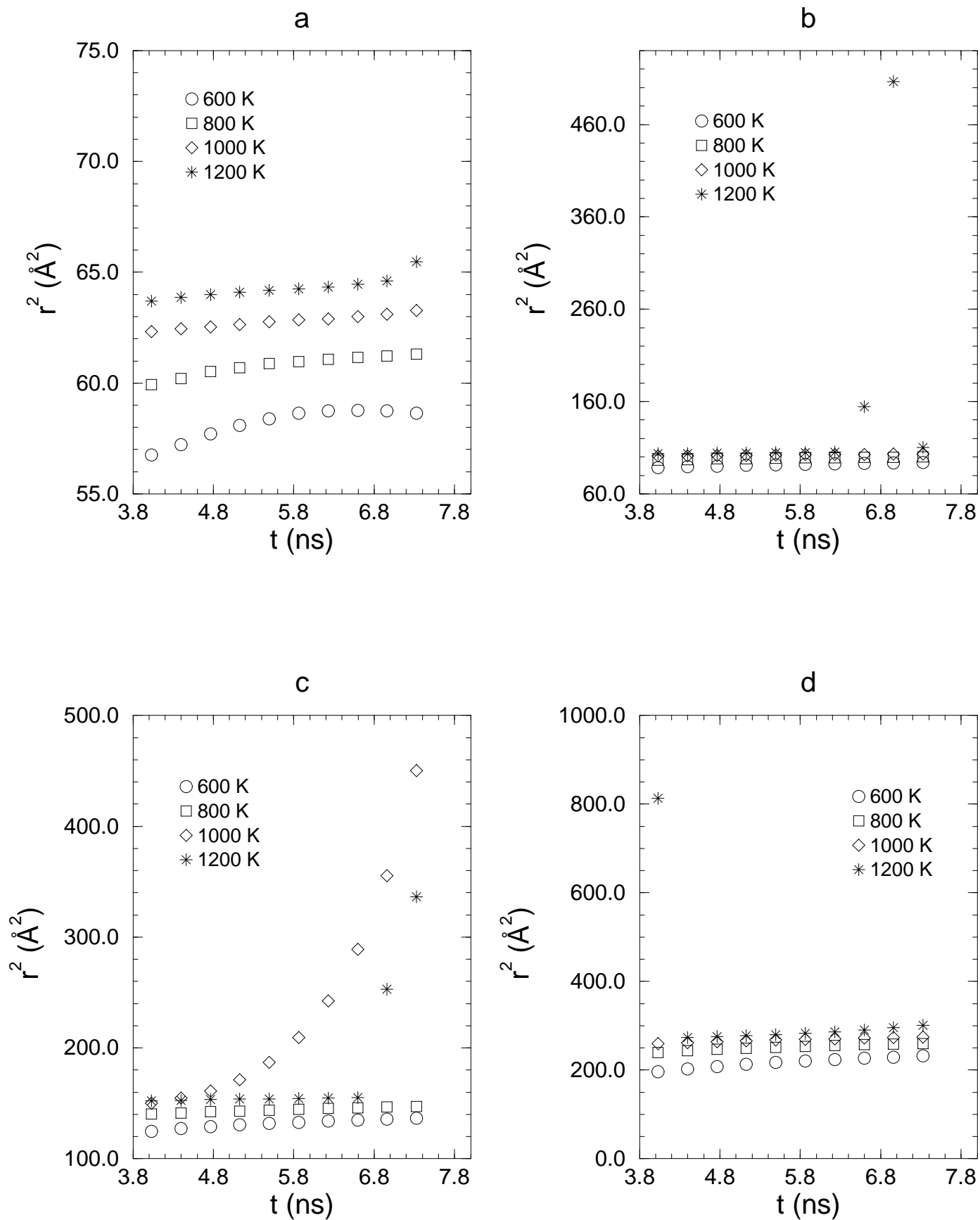


Fig. 2

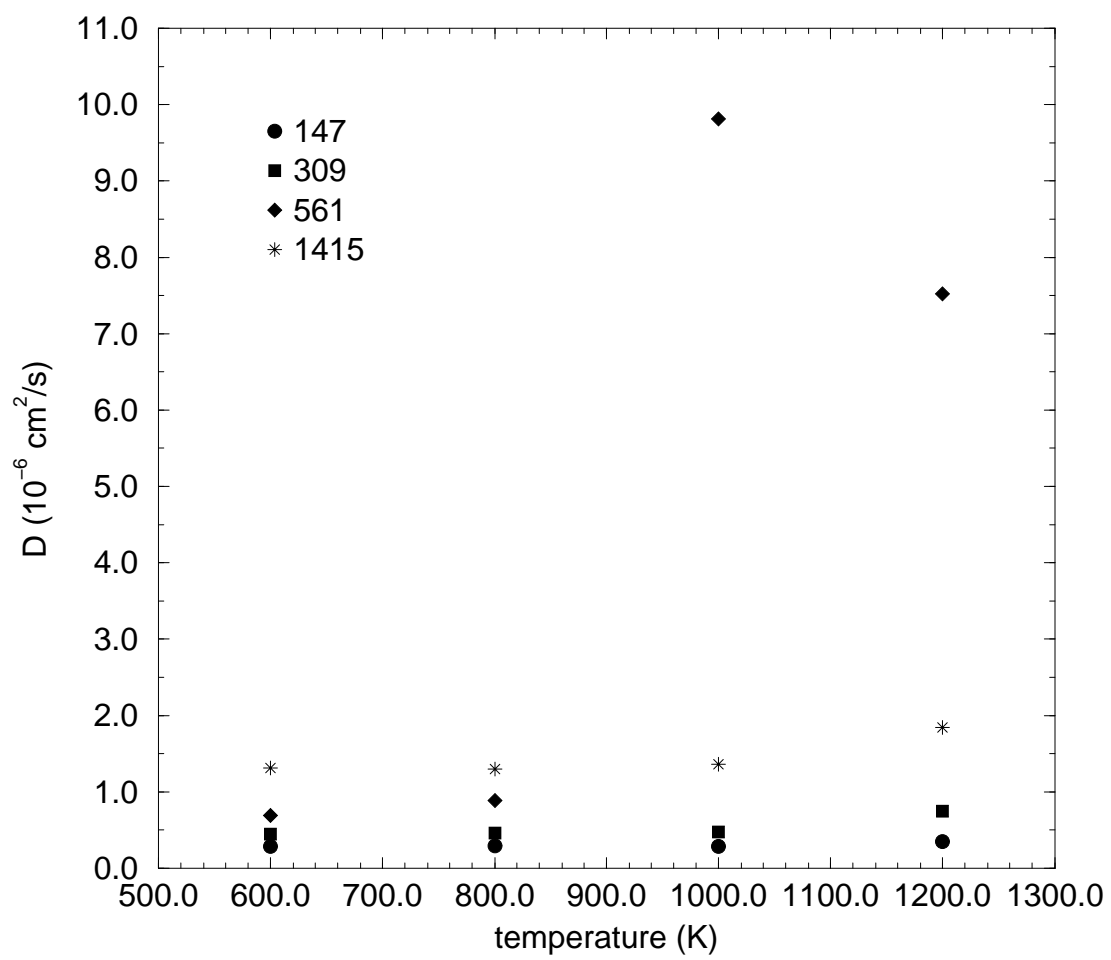


Fig. 3

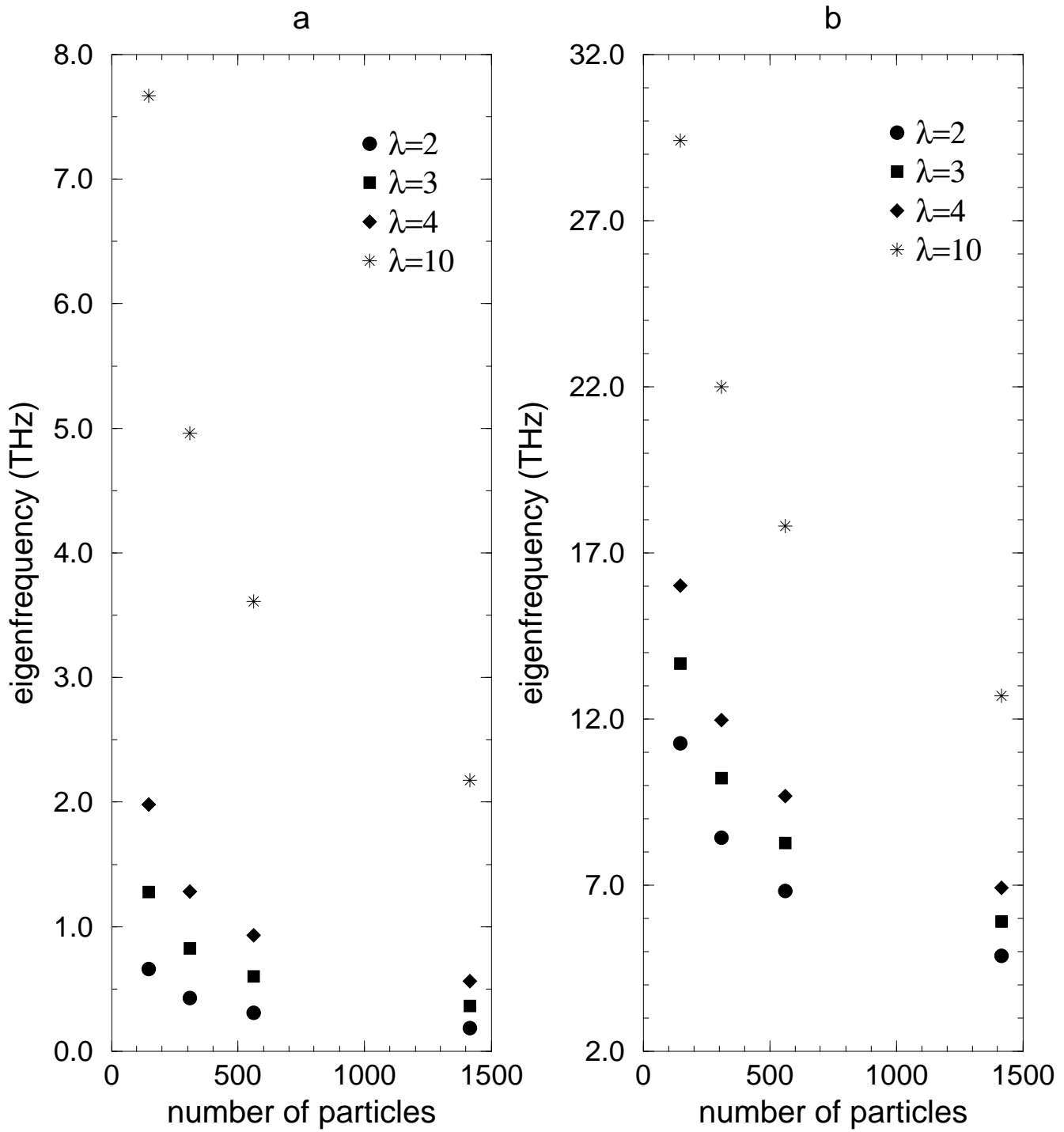


Fig. 4